Vol.16 No.1 (42~49) ACTA SEISMOLOGICA SINICA Jan., 2003

Article ID: 1000-9116(2003)-01-0042-08

An analysis on short-wave components of the global stress field*

HUANG Xi-ying[1,2] (黄玺瑛) WEI Dong-ping[1)] (魏东平) CHEN Qi-fu[3)] (陈棋福)
CHEN Hong[2)] (陈 虹)

1) *Department of Geosciences, Graduate School of Chinese Academy of Sciences, Beijing* 100039, *China*
2) *Institute of Crustal Dynamics, China Seismological Bureau, Beijing* 100085, *China*
3) *Center for Analysis and Prediction, China Seismological Bureau, Beijing* 100036, *China*

Abstract

The 10 920 stress indicators collected so far by the WSM (World Stress Map) project represent the observed orientations of the maximum horizontal principal stress ($s_{H\max}$) in a certain region. Assuming that the long-wave component of $s_{H\max}$ is expressed by the absolute direction of plate motions, we can get the relative orientation and the magnitude of the short-wave component resulted from the local tectonic process or other factors with vector analytical technique. The global surface was divided into basic element bins by 2.5°×2.5° dimensions and the WSM indicators were statistically analyzed for each element by weight coefficient method in order to determine the mean orientation of the stress. We calculated the long-wave component of the global stress field using HS2-NUVEL1 model. The relative magnitude or the direction limitation of short-wave component, which reflect the local contribution to the observed stresses, was determined by the angle between the mean $s_{H\max}$ and the orientation of the long-wave component. The results of this paper show that the contribution of either the long-wave component or the short-wave component is approximately equal to most of the global plates on the basis of the mean effect of the observed stresses. For some of continental regions, the local active tectonics plays an important role in the observed stresses and controls the generation and occurrence of earthquakes.

Key words: stress field; Euler vector; short-wave component
CLC number: P315.72$^+$7 **Document code**: A

Introduction

The intraplate stresses are affected by two types of forces: one is called the first-order stresses (Zoback, 1992) or the long-wave components of stresses, which are closely related to the driving mechanism of the plate motions such as ridge push, continental collision resistance, slab pull (suction) and mantle drag force (Richardson, 1992; WEI, 2000). This type of stress field is characterized by a uniform feature in very large horizontal scale with 50 times or more of the thickness of upper brittle lithosphere, which is about 20 km in general. The other is called the second-order stresses or the short-wave component of stresses. These second-order stress fields can often be associated with the specific geologic or tectonic structures such as the lithospheric flexure, the lateral contrasts of the lithospheric strength, as well as the lateral difference of the lithospheric

* **Received date**: 2002-03-11; **revised date**: 2002-05-13; **accepted date**: 2002-06-19.
Foundation item: MOST contract of 2001BA601B02 and State Natural Science Foundation of China (49804006).
E-mail: Huang@earth.gscas.ac.cn

density. And their patterns typically have the wavelengths ranging from 5 to 10 times the thickness of the brittle upper lithosphere, reflecting the local tectonic feature (Zoback, 1992).

Researchers mainly in geodynamics set about their cooperative efforts to compile and interpret the WSM data on the orientation and relative magnitudes of the tectonic stress field in the Earth′s lithosphere since 1986, and they got the preliminary results described by Zoback and Zoback (1989). Zoback (1992) mentioned that the global stress indicators in the WSM data are the result of the compositive effect of these two types of stresses mentioned-above, and that it provided possibility to estimate the relative magnitude of the local stresses. The latest WSM 2000 release includes 10 920 stress indicators, including the updated prior WSM (1997 version) and new data (http://www-wsm.physik.uni-karlsruhe.de/pub/release_2000/). With the WSM2000 stress data and long-wave components stress deduced from plate motion model, we calculated and discussed the orientation and relative magnitude of short-wave stress related to local tectonics.

1 The source and basic analysis of the observed stress data

In this study, excluding 23 of all the present data due to lack of the orientation information, we took the rest 10 897 WSM2000 stress indicators. The different resources or methods for those data were summarized in Table 1.

Table 1 Basic statistics of the observed data

Stress regime	Focal mechanism	Geology	Well hole	Others	Total
NF	1 238	322	56	45	1 661
NS	282	27	7	12	328
SS	2 290	40	61	70	2 461
TS	278	6	23	32	339
TF	2 289	45	131	122	2 587
U	500	156	337	2 528	3 521
Total	6 877	596	615	2 809	10 897

Those WSM2000 data were ranked by 5 categories, that was A, B, C, D and E from high quality to poor level. The number of data corresponding to the rank A to E was 612, 1 915, 4 854, 2 010 and 1 506, respectively. Here we used the weighted-mean method (Wei, 1997) to calculate the mean orientation of the observed stress indicators, in which their weights were set to be 6, 4, 3, 1 and 0 for the data with the different quality from A to E, respectively.

For a certain area under investigation, the indicators were assigned different weights according to different quality and then were summed and averaged. The mean stress orientation is calculated with the weighted equation

$$\overline{a} = \frac{1}{N}\sum_{i=1}^{N} k_i a_i \tag{1}$$

where $\overline{a}$ is the mean stress orientation, N is the number of indicators, a_i stands for the observed orientation of the i-th stress indicator, and k_i for the corresponding weight. The direction of a stress indicator is recorded clockwise from north with the range of 0° to 180°. It means that an indicator with orientation of 30° is labeled as 270°. In order to avoid confusion for the vector summation, we adopted the double-angle method (Davis, 1986) to process the orientation data by the vector resultant technique in a certain area. The method doubles the participating data azimuths at first, then divides the resultant vector by factor 2 to get the correct summing orientation. We got the mean orientation of the certain area with the double-angle method to represent the mean orientation of $s_{H\max}$ (Wei, 1997; WEI, *et al*, 2001).

The global surface was divided into 10 368 basic element bins by 2.5°×2.5° dimensions, and 1 732 element bins of them were given one and more stress indicators of A to D type in WSM2000 database. The mean observed stress orientation for each bin of them was obtained by the weighted average orientation of the observed indicators, and the Rayleigh test (Davis, 1986) was used to estimate which element bins have well-constrained $s_{H\max}$ orientations. Results showed that 817 bins passed the test at 95% confidence level, accounting for 48% of the whole element bins in total.

2 Long-wave components

By analyzing the observed stress data in the previous WSM data, Zoback (1992), Zoback, *et al* (1989) pointed out that the stress patterns related to the plate drive mechanism could be described as follows. All the $s_{H\max}$ are nearly narrowed in the range of ±15° orientation for the broad regions within most of the plates, which are up to 5 000 km in continental area, and they are closely related to the absolute plate motions. The plate driving forces such as plate boundary forces including ridge push and continent collision are mainly the sources of the long-wave component of intraplate stresses. This is mainly based on the following facts (Zoback, 1992): a) In most places, a uniform stress field exiting in the brittle upper crust layer indicates a large range of the consistent orientation when we made the measurements with different technique for samples in the different crustal depth; b) Stresses in the interior portions are dominantly in compression; c) The active extensional tectonic generally occurs in topographically high areas in both the continents and the oceans; d) Regional consistency of both stress orientations and relative magnitudes permits the definition of broad-scale regional stress provinces, which coincide with physiographic features, particularly with the active tectonical region.

Richardson (1992) compared the absolute plate motions described by the ridge-push torque model with other models as were instanced by AM1-2 (Minster, Jordan, 1978) and HS2-NUVEL1 (Gripp, Gordon, 1990). He also discussed the correlativity among the orientations of plate motions characterized by these models. It is therefore a reasonable assumption that the direction of absolute plate motions indicated the orientation of long-wave components of stress field.

The Euler vector describes the plate motions on the earth surface, and it can be expressed by the polar location of rotating axis (recorded by longitude and latitude) and the rotated velocity of the axis. Giving an Euler vector of a plate, we can calculate the azimuth from the center of a bin including the mean predicted stress indicator to the rotating pole. The azimuth calculated here represents the torque of the force arm while the corresponding tangent direction represents the absolute plate motions.

3 Short-wave components

Let the length of the mean observed stress indicators in each elemental bin be the unified 1 in this paper. In general, if the angle between the long-wave component *OB* and the observed stress *OA* is q ($0° \le q \le 90°$) (see Figure 1), the resultant of *OB* and *BA* is *OA*, which follows the vector resultant principle and the double-angle rule. When the contribution to the observed stress resulted from the long-wave component *OB* and the short-wave component *BA* varies, it equivalents to the movement of point *B* along the segment *OC* from right to left or *vice versa*. The contribution of long-wave component to the stress is less than that of short-wave component when point *B* is moving toward the left. When point *B* overlaps point *O*, its contribution is null because the total contribution to the observed stress is provided by the short-wave component. On the contrary, the long-wave component offers greater contribution than the short wave does when point *B* is moving toward the right. When point *B* moves to the specified point *C* where *OC* is perpendicular to *AC*, the long-wave contribution to the observed stress increases up to the maximum *OC* while the corresponding short-wave component effect decreases down to the minimum *AC*. It is impossible for point *B* to move to point *B′* because the resultant of *OB′* and *AB′* is *OA′* instead of *OA* in this circumstance.

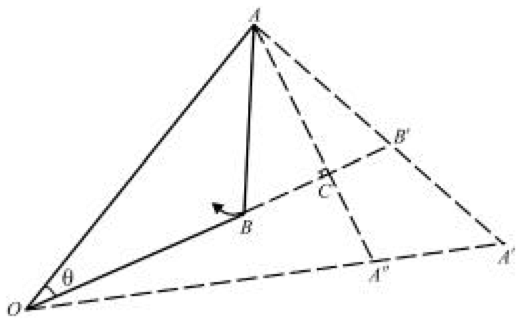

Figure 1 A sketch map of calculating the short-wave component
OA is the observed stress and *OB* is its long-wave component. The angle between *OA* and *OB* is q ($0 \le q \le 90°$), where *BA* is the short-wave component of the observed stress *OA*. See text for detail

The orientation of long-wave component is consistent with the observed stress when q is 0°, and the long-wave component increases up to the maximum value 1 while the corresponding short-wave component is taking the minimum value 0. When q is 90°, the long-wave component takes null value or has no influence on the observed stress while the short-wave component is up to the maximum 1. The contribution of long-wave component and short-wave component thus changes both within the range of 1 to 0 when q varies from 0° to 90°. Especially the lower limit of short-wave components is $\sin q$. In summary, the relative magnitude of short-wave component takes the upper limit 1; and the upper limit of its direction is consistent with the observed stress indicator. The lower limit of short-wave component magnitude is 0 and the lower limit of its direction is perpendicular to the long-wave component. The lower limit of direction is $\sin q$ when its direction is perpendicular to the long-wave components. In this case, the magnitude of the short-wave component is to be the minimum $\sin q$; while to be the maximum 1 when the orientation of the short-wave component is close to the observed stress.

In this study, using the HS2-NUVEL1 global plate motions model (Gripp, Gordon, 1990), we can take the direction of the absolute plate motions of each element bin including the observed indicators by means of its Euler vector. The predicted direction can thus be regarded as the orientation of long-wave components, which strongly correlate with the absolute plate motion direction. These known directions can accordingly determine the short-wave component. Figure 2 shows the global distribution of the minimum global short-wave components with respect to $\sin q$. The size of triangles expresses the magnitudes of $\sin q$. Most of its values are within the range of 0.50~0.60. This fact shows that the contribution of short-wave component and the long-wave component to the observed stress is approximately equivalent. However, for some regions in eastern Eurasian plate, Pacific plate boundary zone, Australian continents, Caribbean plate and eastern Africa, the larger $\sin q$ is corresponding to the stronger influence upon the observed stresses because of their local tectonic activities.

Figure 3 gives the mean value of $\sin q$ for different plates by the HS2-NUVEL1 model. The mean value of $\sin q$ is expressed by $\overline{\sin q}$ as

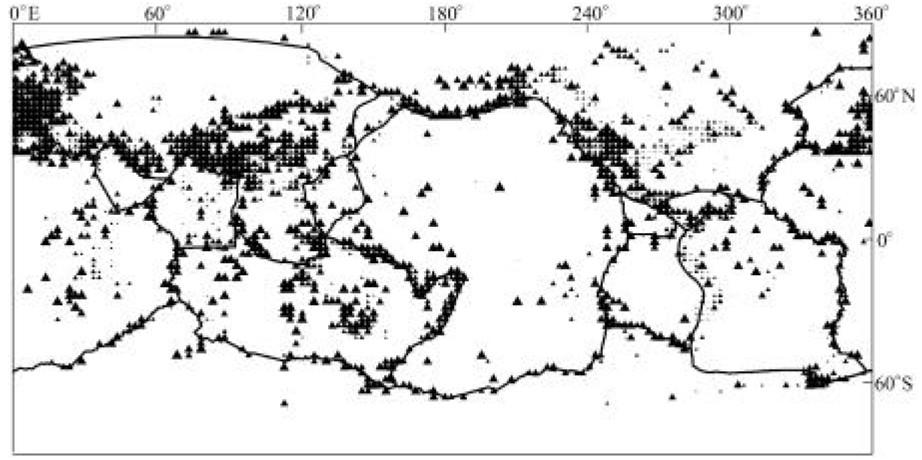

Figure 2 Global distribution of short-wave component based on the HS2-NUVEL1 model (The size of triangles represents the relative contribution of short-wave component to the observed stress field)

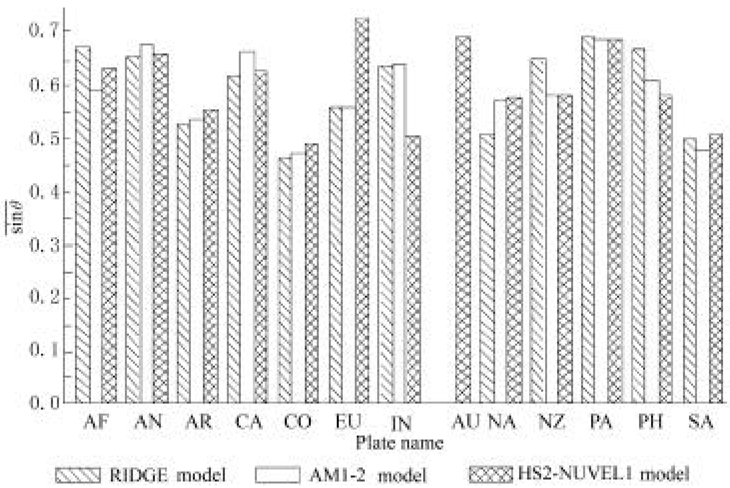

Figure 3 Mean magnitude of global short-wave components for each plate based on the HS2-NUVEL1, the AM1-2 and the Ridge-Push Torque (RIDGE for short) models, respectively

The ordinate denotes the mean contribution of the short-wave component to the observed stress in each plate. Both the AM1-2 and the Ridge-Push Torque model combined the Australian and the Indian plates into a single plate Indo-Australian plate while the HS2-NUVEL1 model regards them as two independent plates. AF: African plate; AN: Antarctic plate; AR: Arabia plate; AU: Australian plate; CA: Caribbean plate; CO: Cocos plate; EU: Eurasian plate; IN: Indian plate; NA: North American plate; NZ: Nazca plate; PA: Pacific plate; PH: Philippine plate: SA: South American plate

$$\overline{\sin\theta} = \frac{1}{N}\sum_{i=1}^{N}\sin\theta \qquad (2)$$

where N is the number of the short-wave component stress indicators contained in each plate. For convenience of comparison, Figure 3 also illustrates the $\overline{\sin\theta}$ based on the AM1-2 model (Minster, Jordan, 1978) and on the Ridge-Push Torque model (Richardson, 1992).

4 Discussion

The contribution resulting from the local stress to the observed stress is dependent on the angle q between the observed stress and the first-order stress, and the latter can also be called the long-wave component of stress. The upper or the lower limits of magnitude of the short-wave component is determined by sin$q$. If the long-wave component is determined by plate motion in a specified region, we can work out the relative contribution of the short-wave component combining with local tectonic information on the basis of the given pattern of observed stresses. Within the orientation variation of the short-wave component range of the upper to the lower limit, we can also investigate the influence resulting from the local tectonic features by combining other data sources, for instance, the geological tectonic information.

Figure 2 demonstrates that several regions, such as west Europe, Qinghai-Xizang plateau, San Andreas fault zone in North America, India Ocean and East Africa rift, are affected intensively by the local tectonics, which are well fitted with the geological fact. In Scandinavia peninsula, Ireland, North Ocean and Alpines, the lithosphere got bent due to the hard pressure from the huge ice cap in Ice Age. When the overlapped ice cap melted in the postglacial period, the lithosphere of this region rebounded gradually as a result of elasticity (Sabadini, *et al*, 1992; Mitrovica, *et al*, 1994; Manga, O'Connell, 1995) and so as that the stress filed is strongly affected by glacial action. The Qinghai-Xizang plateau, San Andreas fault zone, Mid India Ocean ridge and East Africa rift are regions with active local tectonic movements in the meantime. These tectonic activities brought local variation of the thickness of crust and further caused the gravitational anomaly and the crustal inhomogeneity. As a result, the short-wave component contributes more to the observed stresses than the large scale long-wave component does.

We averaged the relative contribution of the short-wave stress and the long-wave stress (see Figure 3). By analyzing the plate driving mechanism by using the observed intraplate stresses in the South American plate, the North American plate and the Philippine plate, the researchers generally give their estimation to the orientation of observed stress field with the fitness less than 60% (Richardson, Reding, 1991; Stefannick, Jurdy, 1992; Pacanovsky, Richardson, 1999; Müller, *et al*, 1992), which coincides with the results based on the mean short-wave intraplate component in the present paper (Figure 3). Comparing the AM1-2 or the Ridge-Push Torque model with the HS2-NUVEL1, we can easily find that the mean effect of short-wave component all over the globe, which is deduced respectively from the above three models, is similar except for that of the Eurasian plate and the Indian plate. Different division of geometry shape of Indian plate causes the resultant deviation about it. The Eurasian plate is a complex instance, with its movement velocity related to the hotspots reference system being very small, typically 5 mm/a. Minster and Jordan (1978), however, pointed out that the uncertainty of the absolute velocity was about 8 mm/a, greater than its movement velocity itself. A dynamical model of the orientation of intraplate stress in the Eurasian plate (Wei, 1997) also showed the estimate of fitness is less than 55%. All of those may imply that the local factors take up 50% of the Eurasian plate stress field. If we adjusted the orientation of short-wave component within its direction limit for different regions, it would be possible to give a better match of local stress patterns. Nevertheless the adjustment scale on global area is difficult to determine because it relies on the local characters of a specified region. The method given in this study provides possibility to get well-fitted stress distribution and pattern of the given tectonic feature in a specific region by changing the proper orientation of the short-wave component of stress field.

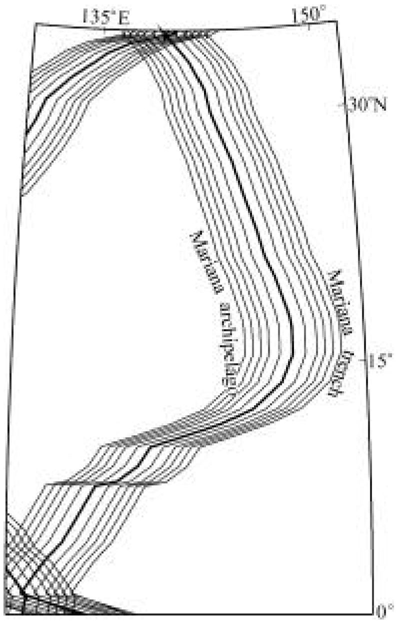

Figure 4 Philippine-Pacific plate boundary band (half bandwidth is from 80 km to 300 km)

The thick line represents the Philippine-Pacific plate boundary known as Mariana trench. The thin lines beside the thick line express the plate boundary band, which indicate the half bandwidth namely 80 km, 150 km, 200 km, 250 km and 300 km from inner to outer

There is quite a large number of WSM2000 data located on plate boundaries. In order to analyze the short-wave component of them comprehensively, plate boundary zone is an important part that must be considered. The movement or state in this zone cannot be well determined by any single plate but by the relative motion of the two-plate-pair. The interaction between the two-plate-pair should be considered in this case. DeMets, *et al* (1990) inverted the relative Euler vector of global shared plate boundary. The long-wave component calculated by the Euler vector denotes the relative motion of two-plate-pair that shared a common boundary. Using the method mentioned above, we can get the short-wave component of the observed stresses along the plate boundary. The short-wave component is the remainder after eliminating long-wave component from the observed stress field. Here we just discuss a segment of typical boundary, an example of convergent Philippine-Pacific plate boundary, because the structure of global plate boundaries is extremely complex. We take account of various widths of plate boundary bands (half bandwidth from 80 km to 300 km) because we are not sure which part of data comes from plate boundary instead of intraplate (see Figure 4). The result shows that the short-wave components $\sin\theta$ in this boundary contribute less than 0.5 no matter which width is adopted (Figure 5). It implicates that the main composition of the stress field near the plate boundary is the long-wave component in this boundary. The stress field is mostly originated by plate driven forces. It is also consistent with the dynamical model by Richardson and Solomon (1979).

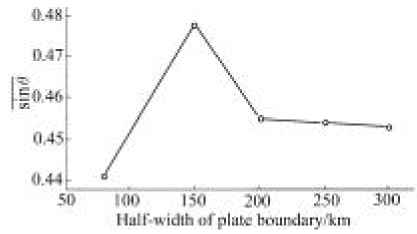

Figure 5 Mean relative contributions of short-wave component corresponding to various plate boundary widths

We have not analyzed and discussed other plate boundaries in detail. It is worthy to work further on the influence of the relative motion between two-plate-pair in dynamical model by all appearances.

Acknowledgments We thank Prof. LIU Bin for reviewing the manuscript. Thanks are given to Dr. P. Wessel and Dr. W. H. F. Smith for providing their software GMT.

References

Davis J C. 1986. *Statistics and Data Analysis in Geology* [M]. New York: John Wiley & Sons Press, 646.

DeMets C, Gordon R G, Argus D, *et al*. 1990. Current plate motions [J]. *Geophys J Int*, **101**: 425~478.

Gripp A E, Gordon R G. 1990. Current plate relative to the hotspots incorporating the NUVEL-1 global plate motion model [J]. *Geophys Res Lett*, **17**: 1 109~1 112.

Manga M, O'Connell J. 1995. The tectosphere and postglacial rebound [J]. *Geophys Res Lett*, **22**: 1 949~1 952.

Minster J B, Jordan T H. 1978. Present-day plate motion [J]. *J Geophys Res*, **83**: 5 331~5 354.

Mitrovica J X, Davis J L, Shapiro I I. 1994. A spectral formalism for computing three-dimensional deformations due to surface loads 2. Present-day glacial isostatic adjustment [J]. *J Geophys Res*, **99**: 7 075~7 101.

Müller B, Zocack M L, Fuchs K, *et al*. 1992. Regional patterns of stress in Europe [J]. *J Geophys Res*, **97**: 11 783~11 803.

Pacanovsky K M, Davis D M, Richardson R M, *et al*. 1999. Intraplate stresses and plate driving forces in the Philippine sea plate [J]. *J Geophys Res*, **104**(B1): 1 095~1 110.

Richardson R M. 1992. Ridge forces, absolute plate motions, and the intraplate stress field [J]. *J Geophys Res*, **97**: 11 739~11 748.

Richardson R M, Reding L M. 1991. North American plate dynamics [J]. *J Geophys Res*, **96**: 12 201~12 223.

Richardson R M, Solomon S C. 1976. Intraplate stress as an indicator of plate tectonic driving forces [J]. *J Geophys Res*, **81**: 1 847~1 856.

Richardson R M, Solomon S C. 1979. Tectonic stress in the plate [J]. *Rev Geophys Space Phys*, **17**: 981~1 019.

Sabadini R C, Giunchi C, Gasperini P, *et al*. 1992. Plate motion and dragging of the upper mantle: Lateral variations of lithospheric thickness and their implications for intraplate deformation [J]. *Geophys Res Lett*, **19**: 749~752.

Stefannick M, Jurdy D M. 1992. Stress observations and driving force models for the South American plate [J]. *J Geophys Res*, **97**: 11 905~11 913.

Wei D P. 1997. *Pseudo-3-D Spherical Modeling of the Intraplate Stresses of the Eurasian Plate: Implications to Plate Dynamics* [D]: [Doctoral Thesis]. Tokyo: Earthquake Research Institute of Tokyo University, 20~23.

WEI Dong-ping. 2000. Asthenospheric static push and its implications to plate dynamics [J]. *J Geomech*, **6**(1): 4~14 (in Chinese).

WEI Dong-ping, ZUO Ru-bin, Seno T. 2001. Weighted statistical analysis of the global observed stress $s_{H\max}$ orientations [J]. *J USTC*, **31**(1): 50~56 (in Chinese).

Zoback M L. 1992. First- and second-order patterns of stress in the lithosphere: The World Stress Map Project [J]. *J Geophys Res*, **97**: 11 703~11 728.

Zoback M L, Zoback M D. 1989. Tectonic stress field of the conterminous United States [J]. *Men Geol Soc Amer*, **172**: 523~539.

Zoback M L, Zoback M D, Adams J, *et al*. 1989. Global patterns of tectonic stress [J]. *Nature*, **341**: 291~298.

Contributors to this issue

YU Xiang-wei (于湘伟) Ph.D. student of Institute of Geophysics, China Seismological Bureau (IGCSB). Graduated at Speciality of Solid Geophysics, Peking University in 1997. Mainly engaged in the researches on topography of near-field earthquakes and earthquake location.

ZOU Zui-hong (邹最红) Graduated from Department of Geophysics, Peking University in 1999. Received her MS degree from Department of Geophysics, Peking University in 2002. Mainly engaged in the researches on seismology and interior structure of the Earth.

ZHANG Chi-jun (张赤军) Professor of Geodesy and Geophysics, Chinese Academy of Sciences. Received his MS degree from the Department of Geodesy, Chinese Academy of Sciences (CAS) in 1967. He has been working on the researches on gravity. Member of Geophysical Society of China and Surveying and Mapping Society of China.

HUANG Xi-ying (黄玺瑛) MS degree candidate majored in geophysics under the joint education of the Crustal Dynamics Institute of China Seismological Bureau and the Graduate School of CAS. Graduated from the College of Disaster Prevention Techniques in 1998. Mainly engaged in the researches on seismicity and plate tectonics.